HHS Public Access

Author manuscript

Nano Lett. Author manuscript; available in PMC 2021 July 08.

Published in final edited form as:

Nano Lett. 2020 July 08; 20(7): 5383–5390. doi:10.1021/acs.nanolett.0c01729.

Untethered Single Cell Grippers for Active Biopsy

Qianru Jin[1,∀], **Yuqian Yang**[1], **Julian A. Jackson**[1], **ChangKyu Yoon**[2,#], **David H. Gracias**[1,2,*]

[1]Department of Chemical and Biomolecular Engineering, Johns Hopkins University, Baltimore, Maryland 21218, USA

[2]Department of Materials Science and Engineering, Johns Hopkins University, Baltimore, Maryland 21218, USA

Abstract

Single cell manipulation is important in biosensing, biorobotics, and quantitative cell analysis. Although microbeads, droplets, and microrobots have been developed previously, it is still challenging to simultaneously excise, capture, and manipulate single cells in a biocompatible manner. Here, we describe untethered single cell grippers, that can be remotely guided and actuated on-demand to actively capture or excise individual or few cells. We describe a novel molding method to micropattern a thermally responsive wax layer for biocompatible motion actuation. The multi-fingered grippers derive their energy from the triggered release of residual differential stress in bilayer hinges composed of silicon oxides. A magnetic layer enables remote guidance through narrow conduits and fixed tissues sections *ex vivo*. Our results provide an important advance in high-throughput single cell scale biopsy tools important to lab-on-a-chip devices, microrobotics, and minimally invasive surgery.

Graphical Abstract

*Corresponding Author: dgracias@jhu.edu.

∀Present address: Disease Biophysics Group, John A. Paulson School of Engineering and Applied Sciences, Harvard University, Cambridge, MA 02138, USA

#Present address: Department of Mechanical Systems Engineering, Sookmyung Women's University, Seoul, 04310, Republic of Korea

Supporting Information

The Supporting Information is available free of charge on the website at DOI, which includes detailed experimental methods, additional data and mechanical analysis (PDF).

Under an option to license agreement between Kley Dom Biomimetics, LLC and the Johns Hopkins University, Prof. D. H. Gracias and the Johns Hopkins University are entitled to royalty distributions related to technology described in the study discussed in this publication. This arrangement has been reviewed and approved by the Johns Hopkins University in accordance with its conflict of interest policies.

Keywords

biomedical engineering; molding; robotics; drug delivery; tissue sampling; genomics; proteomics

Untethered miniaturized devices that can manipulate single cells with high accuracy and reproducibility, hold great promise in robotics, surgery and biomedical engineering.[1–3] Conventional surgical and biopsy devices rely on catheters and endoscopes to navigate through the gastrointestinal, urological, and cardiovascular passageways. However, these processes limit accessibility and often require entry point lesions, cause patient discomfort and collateral damage.[4] Many diseased tissues are highly heterogeneous at the single cell level.[5, 6] Untethered microrobotic devices that can operate at the single cell can open up access to narrow conduits, minimize invasiveness, and enhance the accuracy and efficacy of tissue sampling and surgical interventions.

In vitro biomedical applications such as microdissection, assisted reproductive technology, and somatic cell nuclear transfer could benefit tremendously from single cell manipulators, where high resolution controlled motion could improve efficiency and minimize manual variances.[7, 8] Present-day single cell analysis methods that utilize droplet microfluidics or microbeads to separate cells, are passive and require preparatory procedures for tissue isolation and labeling.[9] Laser-capture microdissection isolates tissues of interest by laser cutting in a microscopic field, albeit with low throughput and relatively compromised sample quality.[9] High-throughput active single cell devices could significantly enhance parallel isolation and analysis of microscale tissues. Furthermore, single cell manipulation could maneuver cells with 3D precision for building multicellular architectures.[10]

Substantial progress has been made in developing single cell sized manipulators, enabled by innovations in miniaturization and energy utilization. Untethered single cell devices provide advantages over wired devices especially in applications which require parallel operation off-chip. However, due to their untethered nature and small size, the energy required for actuation and motion needs to be delivered wirelessly which presents a formidable challenge. Chemically powered microrobots have achieved considerable success *in vitro* and *in vivo*, but they often require highly specialized environment, non-biocompatible solvents and onboard chemical fuels.[11–13] Elsewhere, energy delivered through ultrasound[14] or electromagnetic fields,[15, 16] has been used for cell locomotion, biosensing, tissue cutting, and biomolecular delivery.[8, 16–20] However, their motions are largely limited to translation and rotation, such as pulling or tumbling of isolated cells,[19] or drilling and cleaving of *ex vivo* tissues.[12, 20] This constrained motion limits their applicability to simple tasks and makes it challenging to realize dexterous motions in complex environments such as *in vivo* conduits. Hence, there is a need to develop microrobots that can provide multidimensional motion, movable subunits, swift navigation, and precisely controlled interaction with cells, in a biocompatible environment. Significant technical challenges need to be overcome to create untethered robots with biocompatible and potentially biodegradable materials, to provide energy and guidance from afar, to trigger on-demand actuation, and to integrate these functions at single cell scale.

Here, we address some of these challenges by developing untethered thermo-responsive single cell grippers that employ residual stress powered actuators[21–24] with the introduction of several important advances. First, we integrate a biocompatible thermally responsive layer to enable controlled on-demand actuation. After experimenting with a range of materials, we chose paraffin wax and developed a protocol to micropattern this phase-changing material. As compared to the previously utilized triggers made of photoresist,[24] the bioinert paraffin wax can minimize cytotoxicity. We rationally optimize the design to enable thermally triggered actuation at a cell-friendly biocompatible temperature. Second, we incorporate an iron layer to enable magnetic manipulation from afar. Previous single cell grippers were operated in on-chip arrays, where the gripping motion was controlled by tuning the dissolution rate of a sacrificial layer for passive cell trapping.[21–23] Our newly incorporated functional layers allow the grippers to remain open even upon release from the substrate, so they can be utilized for active on-demand cell capture off-chip. Finally, we demonstrate navigation through complex narrow conduits, targeted capture of single live cells, and biopsy at the micrometer (a few cells) scale. As compared to previously demonstrated grippers that were used to biopsy hundreds of cells,[24] the current gripper size has been scaled down significantly in all dimensions, with a tip-to-tip size of 70 μm when open and 15 μm after folding, and we have demonstrated single (or a few) cell excision with significantly enhanced spatial resolution.

We needed to incorporate a stimuli-responsive trigger to enable on-demand activation of the untethered grippers and chose paraffin wax as the functional material for a variety of reasons. First, wax is chemically and biologically inert and biocompatible[25] and widely used in food products (e.g. cheese) and food processing (e.g. wax paper). Second, technical grade paraffin wax which is a mixture of alkanes with chemical formula of C_nH_{2n+2} ($20<n<40$) exhibits a range of phase-transition temperatures of relevance to biology and the human body.[26] Paraffin has been used previously in microfluidic pumps to provide large thrust, due to its significant solid-to-liquid volume expansion. Previously reported paraffin microfabrication involved the manual deposition of volumes of >1 mm^3 and were somewhat imprecise or complicated.[27] Elsewhere, paraffin micropatterning at lateral dimensions of 400–600 μm was achieved, but the process required several steps of microfabrication with customized specialized equipment.[28]

Here, we developed a novel molding approach to pattern paraffin wax at the microscale, adapted from prior and ongoing efforts in our laboratory.[29] Our approach is straightforward, compatible with conventional microfabrication process, and we can create paraffin micropatterns with lateral dimensions ranging from 1 mm to 10 μm (or potentially smaller depending on the mold size) and uniform thickness in the range of micro- and sub-micrometers. The process flow is illustrated in Figure 1a. Briefly, we first photopatterned and deposited a differentially stressed bilayer composed of silicon monoxide and silicon dioxide. The triggered release of the stored differential stress provides the energy for the gripping motion. Second, we photopatterned and deposited relatively thick segments of silicon dioxide to provide the structural rigidity with a thin iron layer for magnetic response. Finally, for paraffin patterning, we fabricated a mold of a negative photoresist pattern. We then melted the paraffin wax and spin coated it at 140°C while it was a viscous liquid over the photoresist molded patterns. After the silicon wafer cooled down and the wax solidified,

we dissolved the photoresist mold by a gentle wash in acetone and isopropanol. The residual solid paraffin wax took the shape of the negative mold patterns defined by the photoresist.

To visualize the paraffin wax layer which is transparent under visible light illumination, we imaged the grippers by scanning electron microscopy (SEM). Figure 1b shows SEM image of a gripper with the 30 nm thin stress layer (zoom-in in Figure 1c) and rigid panels prior to wax patterning. We patterned the wax layer, which appears dark in color in the SEM image in Figure 1d only on top of the grippers and it completely covers the hinges with a thickness of about 1 μm (Figure 1e). The optical image in Figure 1f shows an array of the grippers after fabrication. We observed that the hinges were transparent in optical images due to the transparency of SiO, SiO_2, and wax; while the rigid arms were opaque due to the iron layer. We note that all steps of the fabrication process are compatible with conventional very large-scale integration (VLSI) and scalable, as seen from the large array of uniformly patterned paraffin on top of the grippers in Figure 1g. It is also noteworthy that our patterning method is versatile and could be applied to other phase changing biocompatible trigger materials. For example, we also successfully patterned food grade butter with a similar resolution (Figure S1).

To realize a functional gripping action at such a small size scale, we needed to carefully optimize the materials and design parameters. The magnitude of the change of Young's moduli of paraffin at different temperatures is critical for the thermal actuation of gripping motion. At low temperature, the rigid paraffin prevents the bilayer hinge from folding. As the temperature increases, the total bending rigidity of the hinge decreases due to the decreased Young' modulus of paraffin. Once the residual stress outweighs the decreasing bending rigidity, the gripper will close. We measured the stress-strain curve of paraffin at 26°C and 37°C by Dynamic Mechanical Analysis (DMA). Figure 2a shows Young's modulus decreased significantly from 6.44 MPa at 26°C to 0.37 MPa at 37°C. These measured values are in qualitative agreement with the range in the literature and the differences can be attributed to differences in the wax composition at different temperatures.[30, 31]

The bending curvature of the multilayered structures depends on the stress, thickness, and mechanical properties of the materials in each layer.[32] The thickness of each layer can be tuned during the deposition steps to achieve the desired fold angles. To determine the optimal paraffin thickness, we adopted an analytical model to predict the fold angle with respect to varying paraffin thicknesses at 26°C and 37°C, using the measured wax modulus and the bilayer stress measured previously,[21] as shown in Figure 2b. For both temperatures, we observed that the fold angle decreases as the paraffin layer thickness increases, due to the increased bending rigidity. At the same paraffin thickness, we observed that the difference between the fold angles at the two temperatures was crucial to determine the working range of the gripper. We found that a paraffin thickness range between 0.5–1 μm was optimal as indicated by the shaded area, i.e. small fold angle at low temperature, and large fold angle at high temperature. A gripper with a thinner paraffin layer will close at the lower temperature, while a gripper with a thicker layer will not close at the higher temperature. Finite element modelling (FEM) in Figure 2c shows folding states of the grippers with two different paraffin thicknesses (0.6 μm and 0.9 μm) and an optimal range of fold angles below (26°C)

and at the trigger (37°C) temperature. Based on the analysis, we chose this paraffin thickness range between 0.6 μm and 0.9 μm in our subsequent experiments.

We experimentally verified the self-folding process with and without the trigger. In Figure 2d, initially all grippers stayed open on the substrate before release. Once, we dissolved the sacrificial layer, all grippers got released from the substrate. Among them, the grippers without the paraffin layer closed instantaneously, but those coated with the paraffin layer remained open. As the temperature increased from 26°C to 37°C, the grippers with the paraffin layer gradually started to close. This study shows that a trigger layer is essential for on-demand thermally responsive actuation at a specific location and time. Moreover, by engineering an actuation temperature of 37°C we ensure that the process is thermally biocompatible. In screening materials for the trigger layer, we found that food-grade butter could also be patterned and used as a trigger layer for thermo-responsive actuation at 37°C (Figure S1).

Scaled down from the previously developed gastrointestinal tract biopsy grippers of 0.25–1 mm size,[24, 33] our single cell grippers feature a tip-to-tip open size of 70 μm, comparable to the size of human arterioles (50–300 μm).[34] To introduce the capability of remote controlled motion, we equipped the grippers with an iron layer for locomotion using a magnetic field. We deposited 100 nm iron at the rigid segments by e-beam evaporation, so the iron layer could provide sufficient magnetization without affecting folding at the hinge. We note that it is a major challenge to move microscale objects at low Reynolds number, due to significant amount of drag experienced by the object at these small scales. Based on the geometry, material properties and an estimated drag coefficient,[33, 35, 36] we calculated that the minimal magnetic field required to power the single cell gripper is on the order of milli T/m (see SI for more details), which is much smaller than the typical gradient field 0.1 T/m used in clinical magnetic resonance imaging (MRI) systems. This feature highlights the potential to use MR for *in vivo* locomotion of the single cell grippers in clinical settings. For simplicity, we used a laboratory bar magnet in our study and demonstrated that we could move the grippers with a velocity up to 100–150 μm/s in PBS buffer in microfluidic channels.

To highlight their small size and the ability to locomote in a complex conduit, we steered an untethered gripper in an *ex vivo* fixed human fallopian tube tissue section (Figure 3a). We could move the gripper to access different locations in the tissue section following a guided path. Figure 3b shows temperature triggered folding at the bifurcation site of the conduits. Upon reaching the bifurcation site (i), we increased the temperature to trigger the gradual close of the gripper (ii-iv). Afterwards, we steered the gripper away along the conduit (Figure 3c). In addition to guidance in biological conduits, we were able to move the grippers in complex microfluidic channels with widths <150 μm, including bifurcating, zigzag, winding and twisted channels, and channels with multiple exits (Figure S2). The ability to navigate through such complex channel geometries highlights accessibility in hard-to-reach spaces which is important for lab-on-a-chip, robotic and *in vivo* applications.

We anticipate that these untethered, thermally responsive grippers can be used to manipulate biological cargo such as single cells with high precision and biocompatibility. We performed capture of a single MDA-MB-231 human breast cancer cell from a distance (Movie S1). We

guided the gripper magnetically and gradually approached the cell periphery (Figure 4a). Upon final position adjustment in Figure 4b (i), we increased the temperature to trigger folding (ii-iii) until the target cell was captured (iv). We were able to capture and transport the cell to any desired position (Figure 4c). Since we designed the grippers so that we can actuate folding around 37°C, the cell capture process is biocompatible. We verified viability using a live/dead assay which shows that the target cell was alive during the actuation process, indicated by the green fluorescence from calcein AM staining (Figure 4d). More details are in the supporting methods and Figure S4. Apart from cells, we verified that the grippers were strong enough to capture and transport significantly stiffer cargo such as 15 μm polystyrene beads (Figure S3), which could be challenging for some soft microrobots. Since the grippers are fabricated using silicon oxides and paraffin, they are chemically inert and can withstand many harsh chemicals and organic solvents. Hence, the grippers are not only able to grip delicate biological cargo but can also be used with a range of alternate cargo in a wide range of chemical environments.

Of relevance to surgery, and in contrast to other passive manipulators such as beads and microdroplets, our grippers have movable appendages which can be used to excise and grasp objects for completing tasks such as biopsies or cell excision from tissue samples. We first applied the grippers for cell excision from a cluster of fibroblasts resembling a laboratory tissue sample. As shown in Figure 5 and Movie S2, we deployed the gripper from a distance (i), moved the gripper to approach the cell cluster (ii), and positioned the gripper at the branch of the cluster (iii). At this point, we began to increase the field temperature when the gripper was positioned properly. The gripper started to close, and successfully captured a few cells at the side (iv). Next, we switched the magnetic field direction, to pull the captured cells away from the cluster (v). We observed that the captured cells were primarily connected to the bulk cluster by association with extracellular matrix. By steering the gripper with the captured cells in different directions, we created a strong twisting motion to separate the cells from the cluster and transport them away (vi). This process highlights the dexterity of motion and the firm grasp of cells by the grippers, which is essential for surgical operations with high precision at single cell length scales. Also, grippers permit visualization of cellular components. Figure 5b shows fluorescence images of, (i) a single cell, and (ii) two cells captured from a cell supension within the folded gripper arms. The suspended cells were previously stained to resolve detailed cellular features including the nuclei (DAPI, blue) and cytoskeleton (microtubules, antibody labeling, green). Figure S5 shows gripping of food-grade chicken liver tissue *ex vivo*.

In summary, we have described a new class of untethered, thermal responsive grippers, that can capture single live cells and perform excision of few cells from cell clumps. Our devices feature extremely small size, controlled actuation and locomotion, dexterous motion, biocompatibility, and high throughput fabrication, providing a new strategy of microscale robotic manipulation with enhanced sophistication.

The small single cell size, scalable fabrication process and possibility for further miniaturization[21] opens up new opportunities for *in vivo* access beyond the GI tract as demonstrated previously,[24] such as human arterioles (50–300 μm), ureters (3–4 mm) and mammary lactiferous ducts (1–2 mm). For *in vivo* applications, grippers triggered at 37°C

would close on thermal equilibration with body temperature. In these cases, if needed, low-temperature storage and delivery could extend the time for autonomous thermal triggering. Alternatively, for on-demand actuation, the grippers could be engineered with wax materials that soften at a slightly higher temperature (e.g. 39–40°C). Since the grippers contain a layer of dense and magnetic iron, they offer the possibility for remote coupling to electromagnetic and acoustic fields and induction heating or high-intensity focused ultrasound could be exploited to remotely and specifically heat heat the grippers and minimize collateral thermal damage.

Our fabrication process is highly reproducible, scalable and compatible with microchip industry for cost-effective fabrication. We note that approximately 200,000 grippers fit on a 3-inch wafer with feasible scale up to millions on larger wafers in semiconductor foundries. The wafer scale fabrication also offers the possibility for future integration of optical or electronic modules,[22, 23] so that biosensing, decision making, and surgical intervention can potentially be performed simultaneously *in situ*. It is also conceivable that antibodies could be patterned to target specific cells for autonomous sampling. Furthermore, with enhanced microfabrication resolution, additional hinges per finger could be incorporated for more complex motions including opening up to release captured objects. Finally, the use of bioresorbable films such as SiO, SiO_2 and Fe[37, 38] offer the possibility to create devices that could degrade within the human body which is important from a safety perspective.

Supplementary Material

Refer to Web version on PubMed Central for supplementary material.

ACKNOWLEDGMENTS

We would like to thank Dr. Evin Gultepe and YooSun Shim for helpful suggestions related to the micropatterning of paraffin wax and to Dr. Arijit Ghosh for discussions on magnetic gradient field estimation. We acknowledge support from the National Science Foundation NSF CMMI 1635443. We also acknowledge support from the National Institute of Biomedical Imaging and Bioengineering (NIBIB) of the National Institutes of Health (NIH) under award number R01EB017742. The content is solely the responsibility of the authors and does not necessarily represent the official views of the National Institutes of Health.

References

1. Ceylan H; Giltinan J; Kozielski K; Sitti M Mobile microrobots for bioengineering applications. Lab. Chip 2017, 17, 1705–1724. [PubMed: 28480466]
2. Avila BE-FD; Gao W; Karshalev E; Zhang L; Wang J Cell-Like Micromotors. Acc. Chem. Res 2018, 51, 1901–1910. [PubMed: 30074758]
3. Soto F; Chrostowski R Frontiers of Medical Micro/Nanorobotics: in vivo Applications and Commercialization Perspectives Toward Clinical Uses. Front. Bioeng. Biotechnol 2018, 6, 170. [PubMed: 30488033]
4. Nelson BJ; Kaliakatsos IK; Abbott JJ Microrobots for minimally invasive medicine. Annu. Rev. Biomed. Eng 2010, 12, 55–85. [PubMed: 20415589]
5. Lawson DA; Bhakta NR; Kessenbrock K; Prummel KD; Yu Y; Takai K; Zhou A; Eyob H; Balakrishnan S; Wang CY; Yaswen P; Goga A; Werb Z Single-cell analysis reveals a stem-cell program in human metastatic breast cancer cells. Nature 2015, 526, 131–135. [PubMed: 26416748]
6. Park J; Shrestha R; Qiu C; Kondo A; Huang S; Werth M; Li M; Barasch J; Susztak K Single-cell transcriptomics of the mouse kidney reveals potential cellular targets of kidney disease. Science 2018, 360, 758–763. [PubMed: 29622724]

7. Ichikawa A; Sakuma S; Sugita M; Shoda T; Tamakoshi T; Akagi S; Arai F On-chip enucleation of an oocyte by untethered microrobots. J. Micromech. Microeng 2014, 24, 095004.
8. Medina-Sánchez M; Schwarz L; Meyer AK; Hebenstreit F; Schmidt OG Cellular cargo delivery: Toward assisted fertilization by sperm-carrying micromotors. Nano Lett. 2016, 16, 555–561. [PubMed: 26699202]
9. Matuła K; Rivello F; Huck WT Single-Cell Analysis Using Droplet Microfluidics. Adv. Biosyst 2020, 4, 1900188.
10. Chen P; Güven S; Usta OB; Yarmush ML; Demirci U Biotunable acoustic node assembly of organoids. Adv. Healthcare Mater 2015, 4, 1937–1943.
11. Ávila BE-FD; Angsantikul P; Li J; Lopez-Ramirez MA; Ramírez-Herrera DE; Thamphiwatana S; Chen C; Delezuk J; Samakapiruk R; Ramez V Micromotor-enabled active drug delivery for in vivo treatment of stomach infection. Nat. Commun 2017, 8, 1–9. [PubMed: 28232747]
12. Kagan D; Benchimol MJ; Claussen JC; Chuluun-Erdene E; Esener S; Wang J Acoustic droplet vaporization and propulsion of perfluorocarbon-loaded microbullets for targeted tissue penetration and deformation. Angew. Chem., Int. Ed. Engl 2012, 51, 7519–7522. [PubMed: 22692791]
13. Solovev AA; Xi W; Gracias DH; Harazim SM; Deneke C; Sanchez S; Schmidt OG Self-propelled nanotools. ACS Nano 2012, 6, 1751–1756. [PubMed: 22233271]
14. Wang W; Li S; Mair L; Ahmed S; Huang TJ; Mallouk TE Acoustic propulsion of nanorod motors inside living cells. Angew. Chem., Int. Ed. Engl 2014, 53, 3201–3204. [PubMed: 24677393]
15. Xu X; Kim K; Li H; Fan DL Ordered arrays of Raman nanosensors for ultrasensitive and location predictable biochemical detection. Adv. Mater 2012, 24, 5457–5463. [PubMed: 22887635]
16. Fan D; Yin Z; Cheong R; Zhu FQ; Cammarata RC; Chien C; Levchenko A Subcellular-resolution delivery of a cytokine through precisely manipulated nanowires. Nat. Nanotechnol 2010, 5, 545. [PubMed: 20543835]
17. Chatzipirpiridis G; Ergeneman O; Pokki J; Ullrich F; Fusco S; Ortega JA; Sivaraman KM; Nelson BJ; Pané S Electroforming of implantable tubular magnetic microrobots for wireless ophthalmologic applications. Adv. Healthcare Mater 2015, 4, 209–214.
18. Pal M; Somalwar N; Singh A; Bhat R; Eswarappa SM; Saini DK; Ghosh A Maneuverability of magnetic nanomotors inside living cells. Adv. Mater 2018, 30, 1800429.
19. Sakar MS; Steager EB; Kim DH; Kim MJ; Pappas GJ; Kumar V Single cell manipulation using ferromagnetic composite microtransporters. Appl. Phys. Lett 2010, 96, 043705.
20. Xi W; Solovev AA; Ananth AN; Gracias DH; Sanchez S; Schmidt OG Rolled-up magnetic microdrillers: towards remotely controlled minimally invasive surgery. Nanoscale 2013, 5, 1294–1297. [PubMed: 23154823]
21. Malachowski K; Jamal M; Jin Q; Polat B; Morris CJ; Gracias DH Self-folding single cell grippers. Nano Lett. 2014, 14, 4164–4170. [PubMed: 24937214]
22. Jin Q; Li M; Polat B; Paidi SK; Dai A; Zhang A; Pagaduan JV; Barman I; Gracias DH Mechanical Trap Surface-Enhanced Raman Spectroscopy for Three-Dimensional Surface Molecular Imaging of Single Live Cells. Angew. Chem., Int. Ed. Engl 2017, 56, 3822–3826. [PubMed: 28199758]
23. Cools J; Jin Q; Yoon E; Alba Burbano D; Luo Z; Cuypers D; Callewaert G; Braeken D; Gracias DH A Micropatterned Multielectrode Shell for 3D Spatiotemporal Recording from Live Cells. Adv. Sci 2018, 5, 1700731.
24. Gultepe E; Randhawa JS; Kadam S; Yamanaka S; Selaru FM; Shin EJ; Kalloo AN; Gracias DH Biopsy with thermally-responsive untethered microtools. Adv. Mater 2013, 25, 514–519. [PubMed: 23047708]
25. Noti A; Grob K; Biedermann M; Deiss U; Brüschweiler BJ Exposure of babies to C15–C45 mineral paraffins from human milk and breast salves. Regul. Toxicol. Pharmacol 2003, 38, 317–325. [PubMed: 14623482]
26. Hyun DC; Levinson NS; Jeong U; Xia Y Emerging applications of phase-change materials (PCMs): teaching an old dog new tricks. Angew. Chem., Int. Ed. Engl 2014, 53, 3780–3795. [PubMed: 24470287]
27. Liu RH; Bonanno J; Yang J; Lenigk R; Grodzinski P Single-use, thermally actuated paraffin valves for microfluidic applications. Sens. Actuators, B 2004, 98, 328–336.

28. Carlen E; Mastrangelo C In Paraffin actuated surface micromachined valves, Proceedings IEEE Thirteenth Annual International Conference on Micro Electro Mechanical Systems, Miyazaki, Japan, Jan 23–27, 2000; IEEE: Piscataway, NJ, 2000.
29. Shim Y Diagnostics and Therapeutics Using Untethered Microgrippers. M.S.E. Thesis, Johns Hopkins University, Baltimore, MD, 2013.
30. Craig R; Eick J; Peyton F Strength properties of waxes at various temperatures and their practical application. J. Dent. Res 1967, 46, 300–305. [PubMed: 5226403]
31. Nakano T; Yoshida K; Ikeda S; Oura H; Fukuda T; Matsuda T; Negoro M; Arai F In Fabrication of Transparent Arteriole Membrane Models, Proceedings of 2008 International Symposium on Micro-NanoMechatronics and Human Science, Nagoya, Japan, Nov 6–9, 2008 IEEE: Piskataway, NJ, 2008.
32. Nikishkov GP Curvature estimation for multilayer hinged structures with initial strains. J. Appl. Phys 2003, 94, 5333–5336.
33. Ongaro F; Scheggi S; Ghosh A; Denasi A; Gracias DH; Misra S Design, characterization and control of thermally-responsive and magnetically-actuated micro-grippers at the air-water interface. PloS One 2017, 12.
34. Intengan HD; Schiffrin EL Structure and mechanical properties of resistance arteries in hypertension: role of adhesion molecules and extracellular matrix determinants. Hypertension 2000, 36, 312–318. [PubMed: 10988257]
35. Jones A; Knudsen JG Drag coefficients at low Reynolds numbers for flow past immersed bodies. AIChE J. 1961, 7, 20–25.
36. Utsushikawa Y; Niizuma K The saturation magnetization of Fe-N films prepared by nitriding treatment in N2 plasma. J. Alloys Compd 1995, 222, 188–192.
37. Hwang S-W; Tao H; Kim D-H; Cheng H; Song J-K; Rill E; Brenckle MA; Panilaitis B; Won SM; Kim Y-S A physically transient form of silicon electronics. Science 2012, 337, 1640–1644. [PubMed: 23019646]
38. Kang SK; Hwang SW; Cheng H; Yu S; Kim BH; Kim JH; Huang Y; Rogers JA Dissolution behaviors and applications of silicon oxides and nitrides in transient electronics. Adv. Funct. Mater 2014, 24, 4427–4434.

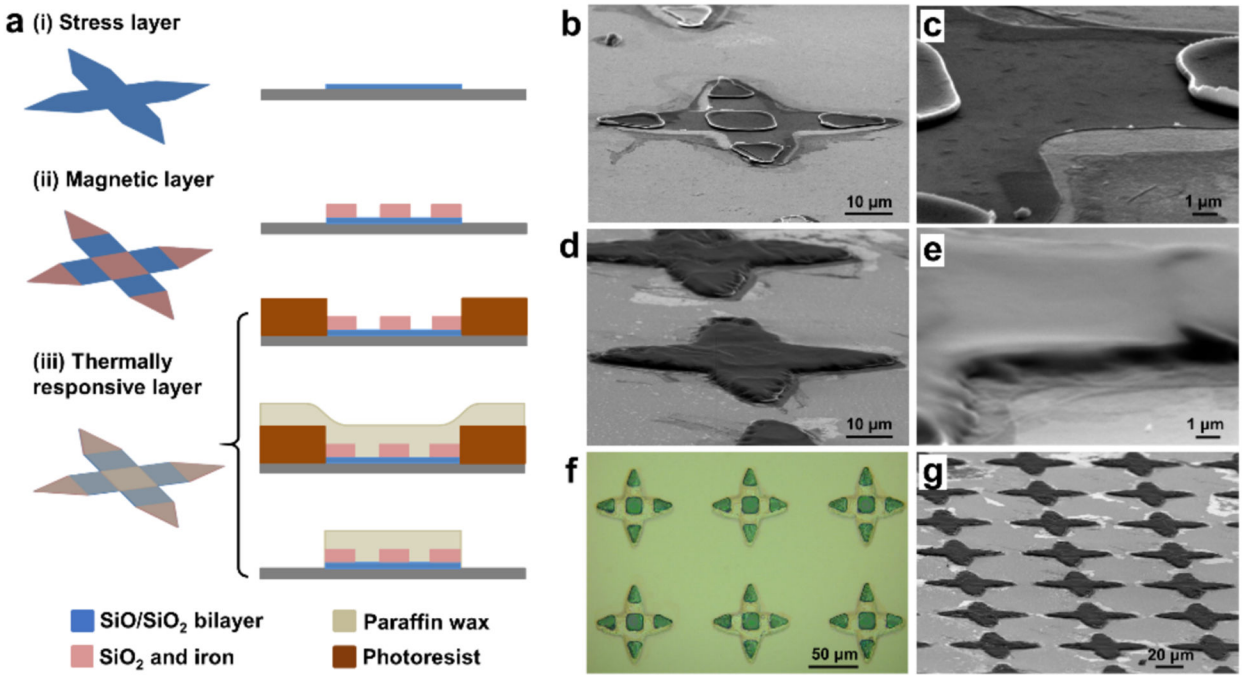

Figure 1. Fabrication of single cell grippers with magnetic response and a thermally responsive trigger.

(a) Schematics of the fabrication process for single cell grippers which include the following steps, (i) photolithography and deposition of the silicon monoxide (SiO) and silicon dioxide (SiO2) bilayer as the stress layer; (ii) photolithography and deposition of silicon dioxide and iron as the rigid segments for magnetic response; (iii) patterning of the paraffin layer by photoresist molding, paraffin spin coating and lift-off. **(b-c)** SEM image of (b) a gripper without the paraffin layer, and (c) a zoom-in view at the hinge. **(d-e)** SEM image of (d) a gripper with paraffin layer, and (e) a zoom-in view at the hinge. **(f)** Optical image of an array of single cell grippers, with rigid iron segments and transparent (SiO/SiO2) bilayer hinges; the transparent paraffin layer covers the entire gripper. **(g)** SEM image of a large array of grippers with a patterned paraffin layer on top.

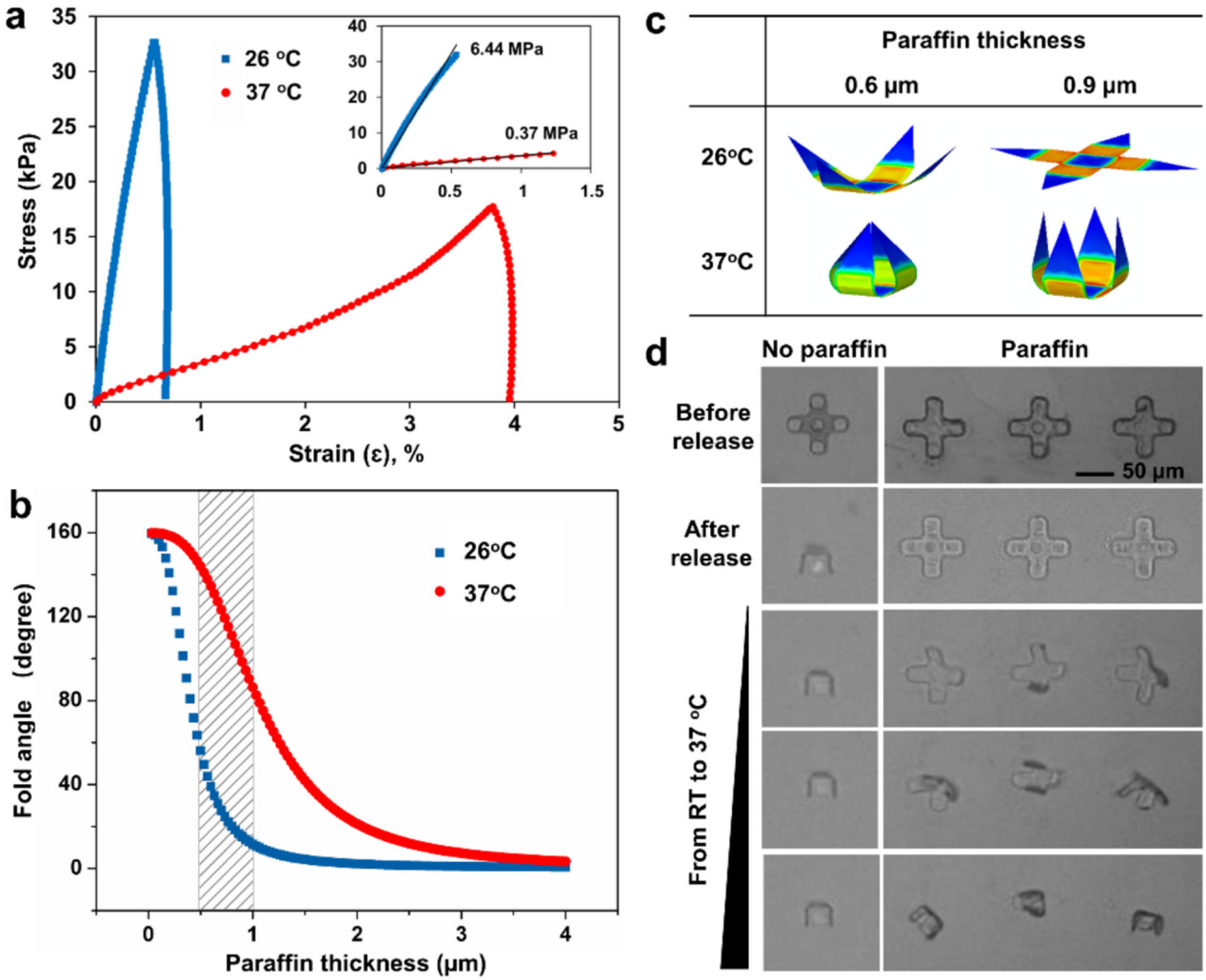

Figure 2. Mechanical characteristics of the paraffin wax trigger and fold angle optimization of the single cell grippers.

(a) Stress/strain curve for paraffin wax at temperatures of 26°C and 37°C based on DMA measurement. Inset shows the initial linear range. **(b)** Analytical study of the fold angle of single cell grippers as a function of paraffin thickness at 26°C and 37°C, based on the analytical solution from reference.[32] **(c)** Finite element simulation snapshots of single cell grippers with two different wax thicknesses at 26°C and 37°C. **(d)** Folding process of single cell grippers before release, after release, and during the heating process from room temperature to 37°C. The gripper in the left column did not have paraffin layer; the three grippers in the right column had paraffin layer on top as indicated by the dark edge and coating all over the gripper in the first row.

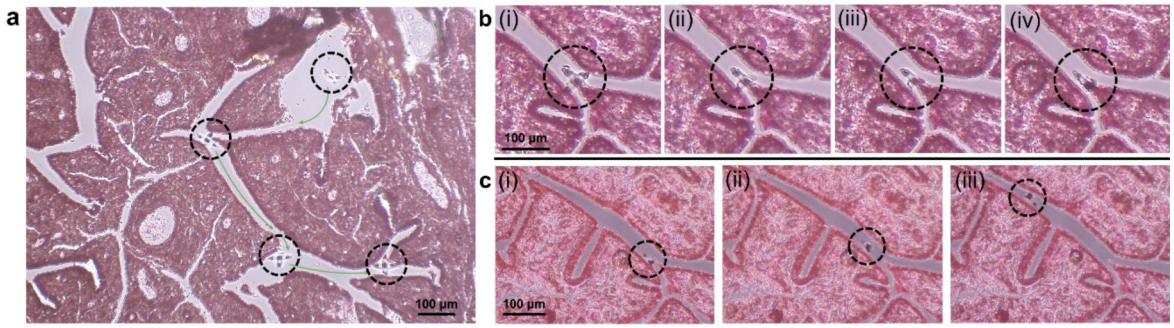

Figure 3. Guided navigation of a single cell gripper through fixed human fallopian tube tissue.

(a) An open gripper moving in a slice of *ex vivo* human fallopian tube tissue, guided by a gradient magnetic field. **(b)** (i-iv) Optical snapshots show the gripper actuation upon temperature increase at the bifurcation site within the biological conduits. **(c)** (i-iii) Optical snapshots show the closed gripper being navigated leaving the biological conduit. The hematoxylin and eosin (H&E) stained tissue slice was dissembled from a commercially available microscope slide.

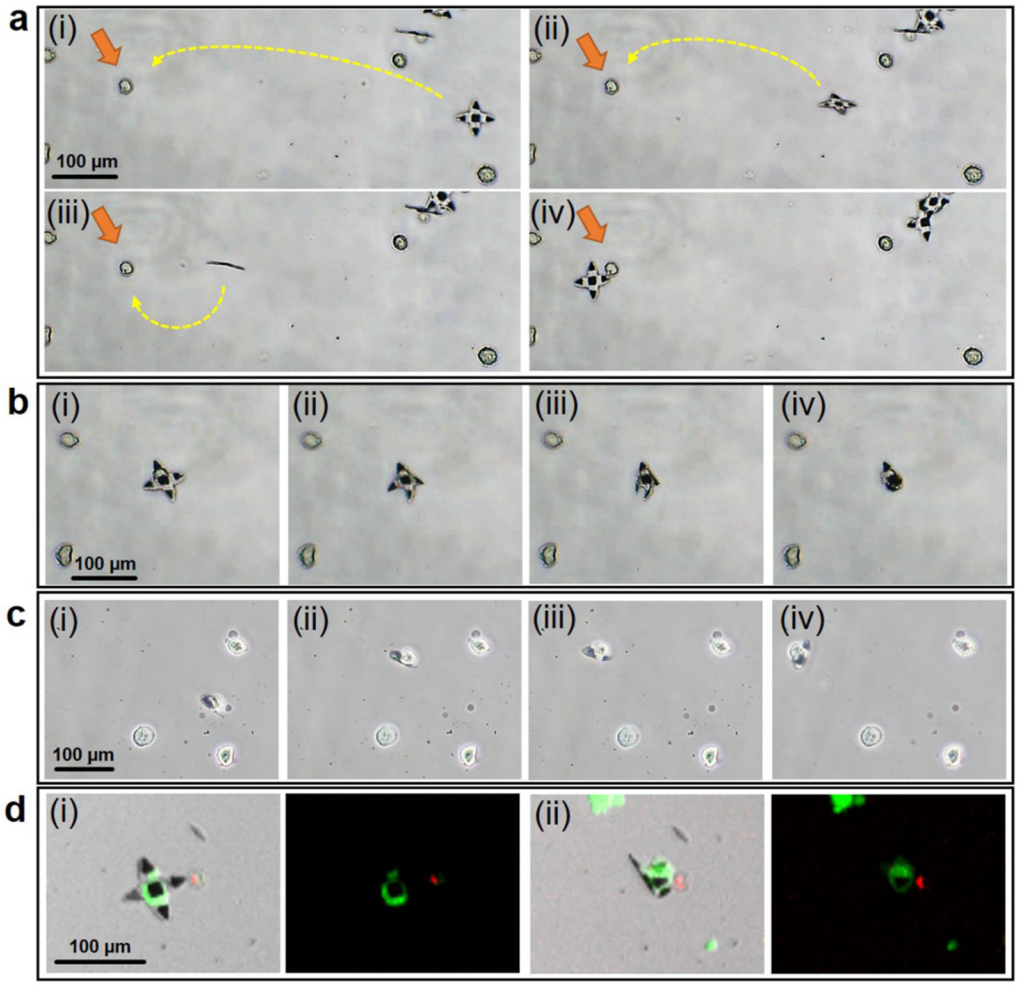

Figure 4. Approach and capture of a single cell using the thermo-responsive grippers.

(a) (i-iv) Optical images show a 70 μm tip-to-tip sized gripper being guided by magnetic field and approaching a targeted cell from a distance. **(b)** (i-iv) On reaching the targeted cell, the gripper was actuated by increasing field temperature. **(c)** (i-iv) The gripper captured the single cell, and carried the cell away guided by magnetic field. **(d)** A Live/Dead assay was performed on the cells (i) before and (ii) after the actuation of grippers. The green fluorescence indicates that the cell was alive after capture. Green and red fluorescence resulted from staining by calcein AM (live, green) and ethidium homodimer (dead, red). Suspended MDA-MB-231 cells were used in this experiment.

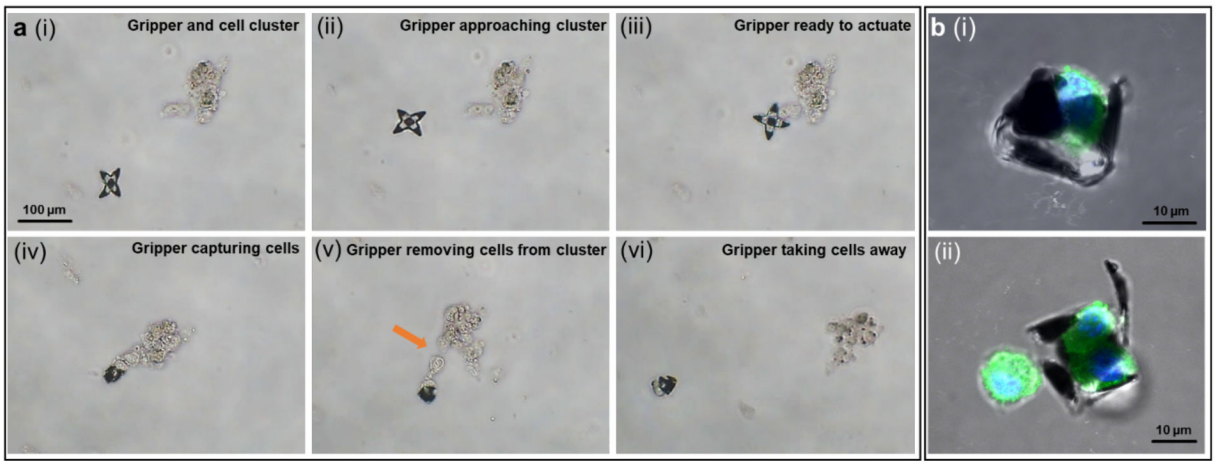

Figure 5. Few-cell biopsy from a cell cluster and visualization of cellular components of captured suspended cells.

(a) The process of a gripper capturing and excising cells from a cell cluster in the following steps, (i) a gripper and a cell cluster at a distance; (ii) the gripper approached the cell cluster guided by magnetic field; (iii) the gripper reached the desired location; (iv) upon temperature increase, the gripper grasped a few cells; (v) the gripper was dragging the captured cells away from the cluster by changing directions of magnetic field; (vi) the gripper successfully excised cells and moved them away. **(b)** Immunofluorescence images of suspended fibroblast cells captured by the grippers: (i) side view of a captured single cell, (ii) two cells captured inside a gripper. Cells were fixed and stained for nuclei (DAPI, blue), and β-tubulin (antibody labeling, green).